Sub-100 µs Settling Time and Low Voltage Operation for Gimbal-less Two-Axis Scanners

Veljko Milanović and Kenneth Castelino*

Adriatic Research Institute
828 San Pablo Ave., Ste. 115E, Berkeley, CA 94706
veljko@adriaticresearch.org

*Department of Mechanical Engineering
University of California at Berkeley
Berkeley, CA 94720

Abstract - We demonstrate high speed point-to-point laser scanning with gimbal-less two-axis micromirror scanners that were previously demonstrated [1],[2]. We apply and compare several different open-loop and closed-loop control techniques on monolithic single-crystal silicon micromirrors of 0.6 mm diameter and on a high fill-factor tip-tilt-piston device of 0.8x0.8 mm^2. Both in open-loop and closed-loop methodology very broadband operation beyond the first resonance is possible which results in very fast settling times. The fastest open-loop result of 96 μs settling time (from 2° to within 1% of final value of 4° of scan angle) was obtained by combining an "inverse transfer function" filter and a square root function. Fastest closed-loop settling-time with optical feedback and PD control was 92 μs. Furthermore, we utilize a simple and robust methodology for low-voltage (<1V rms) operation of the scanner system and demonstrate various vector display examples by driving such systems from a laptop's audio port.

Keywords**:** Two-axis micromirror, settling time, transient response, gimbal-less, optical MEMS.

INTRODUCTION

MEMS micromirror devices generally have high mechanical Q (50 to 100) and micromirror position is usually a non-linear function of applied voltage, especially in the case of gap-closing actuators, which makes their actuation and control challenging. The transient device performance and control schemes for optimizing device characteristics such as settling time, which are critical in most applications, are not often reported. Schemes for closed-loop control of micromirrors using PID or adaptive controllers [3] have been proposed, which alleviate above difficulties but require position sensors and often complex circuitry. Open-loop control schemes using various filters and pulse-shaping are simpler to implement and may be sufficient for many applications. For example, Hah *et al* [4] reported a 120 μs settling time for small micromirrors (137 x 120 μm^2). Yamamoto *et al* [5] used a filter based on inverse-transfer function calculations of the mirror dynamics to eliminate vibration around the resonant frequency, thereby reducing the settling time of their device to 3 ms. Their result was reported for a 0.6 mm diameter micromirror which is an sufficient aperture size for most applications and is identical to the size of our devices. On the other hand, closed-loop galvanometer-based optical scanners are well characterized and typically achieve settling times on the order of hundreds of microseconds [6]. Their main disadvantages are the very high power requirement and their large size.

DEVICE MODEL AND CONTROL METHODS

Our gimbal-less two-axis scanners (Fig. 1a,b) are based on monolithic, vertical combdrive actuators which provide a nearly constant force/torque with position up to ~10° of mechanical rotation [7]. Hence, the only non-linearity derives from the electrostatic actuation force relationship $F \sim V^2$. After extensive characterization of several device designs, we developed a simple model for the device operation as shown in Fig. 1c. This model predicts device behavior very accurately for 0° to ~10° of rotation, at which point the combfingers begin to approach full-engagement and behavior begins to deviate from the model. This simple model requires only three parameters for system identification of an individual device (mechanical natural frequency ω_n, damping factor ζ, and gain *K1*K2* in Fig. 1c.) We used this model to analyze various actuation and control schemes which were subsequently experimentally verified. The simplest scheme which gives surprisingly good performance is to implement the devices in open-loop, and to pre-filter input signals with adequate low-pass filters ("LPF") to prevent excitation of resonance. The second open-loop scheme (inverse-square-root, "ISR") schematically shown in Fig. 2a in essence inverts the device model of Fig. 1c and computes an almost optimal input waveform with system bandwidth limitations represented by the LPF block. The third scheme uses closed-loop PD ("CLPD") control with a position sensitive diode for feedback (Fig. 2a,b.) The best settling time in open-loop measured 96 μs (ISR method, Fig. 2c) and the best result for closed-loop measured 92 μs (CLPD method,) both for Device 2. Fig. 3a tabulates the settling times of all 3 devices measured with different schemes.

LOW VOLTAGE OPERATION

The devices require extremely low power (< 1mW) to operate at full speed as compared to the galvanometer-based laser scanners. This allows us to utilize simple techniques to significantly reduce operating voltages in the laser scanner demonstration system (Fig. 4.) Since the actuators respond to $F \sim v^2(t)$, the rms value of the applied ac signal produces the equivalent result as dc voltage required for a given angle. For carrier frequency (e.g. 17 kHz) much greater than $\omega_n / 2\pi$, the mechanical operation is without jitter and follows the envelope of the carrier. The main advantage is that a simple audio-frequency transformer can be used to amplify the ac voltage (Fig. 4.) Our low cost demo utilizes a laptop audio port as a function generator, to produce ~$2V_{pp}$ signals at audio frequencies. The output voltage is raised sufficiently to operate an actuator to full 20° deflection using a 100:1 audio transformer. A couple of vector scanned patterns generated by our device are shown in Fig. 3b

CONCLUSIONS

By combining the open-loop broadband control methods and low-voltage transformer-based operation, we have integrated a complete two-axis laser scanner system into a small box (Fig. 4a) that requires two channels of <1 V rms at <1 mW for high performance two-axis point-to-point and vector scanning.

[1] V. Milanović, *et al*, "Tip-Tilt-Piston Actuators for High Fill-Factor Micromirror Arrays," *Solid State Sensor and Actuator Workshop*, Hilton Head, SC, Jun. 6-10, 2004.

[2] V. Milanović, *et al*, "Monolithic High Aspect Ratio Two-axis Optical Scanner in SOI," *Int. MEMS Symp. 2003*, Kyoto, Japan, pp. 255-258, 2003.

[3] K.-M. Liao, *et al*, "Closed-Loop Adaptive Control for Torsional Micromirrors," *MOEMS and Miniaturized Systems IV*, Proc. of SPIE Vol. 5346, pp. 184-192, Jan. 2004.

[4] D. Hah, et. al., "Low-Voltage, Large-Scan Angle MEMS Micromirror Arrays With Hidden Vertical Comb-Drive Actuators", J. MEMS, Vol. 13, No. 2, pp. 279-289, 2004.

[5] T. Yamamoto, et. al., "A Three-Dimensional MEMS Optical Switching Module Having 100 Input and 100 Output Ports, IEEE Photonics Tech. Lett., vol. 15, no. 10, Oct. 2003, pp 1360-62.

[6] Cambridge Technology, Inc., Cambridge, MA 02138.

[7] V. Milanović, "Multilevel-Beam SOI-MEMS Fabrication and Applications," *J. of MEMS*, vol. 13, no. 1, pp. 19-30, Feb. 2004.

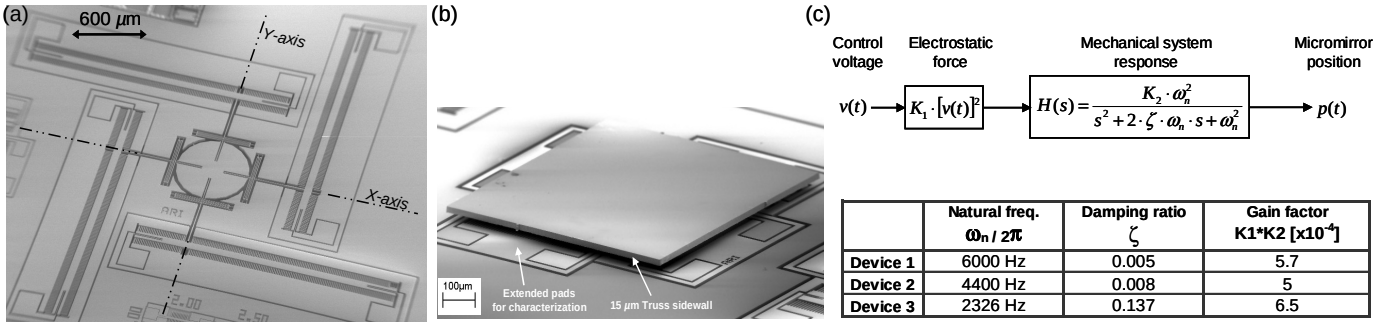

	Natural freq. $\omega_n / 2\pi$	Damping ratio ζ	Gain factor K1*K2 [x10^{-4}]
Device 1	6000 Hz	0.005	5.7
Device 2	4400 Hz	0.008	5
Device 3	2326 Hz	0.137	6.5

Figure 1. Gimbal-less two-axis micromirror scanners: (a) SEM of a typical monolithic device with a 600 μm diameter micromirror, such as Device 1 and Device 2 (b) a tip-tilt-piston actuator with a bonded silicon micromirror for high fill-factor arrays (Device 3) (c) non-linear model of the devices' response characteristics with the model parameters for the three devices in this work extracted from measurements. Note that the high fill-factor device has significantly larger damping ratio due to the bonded micromirror's squeeze-film damping.

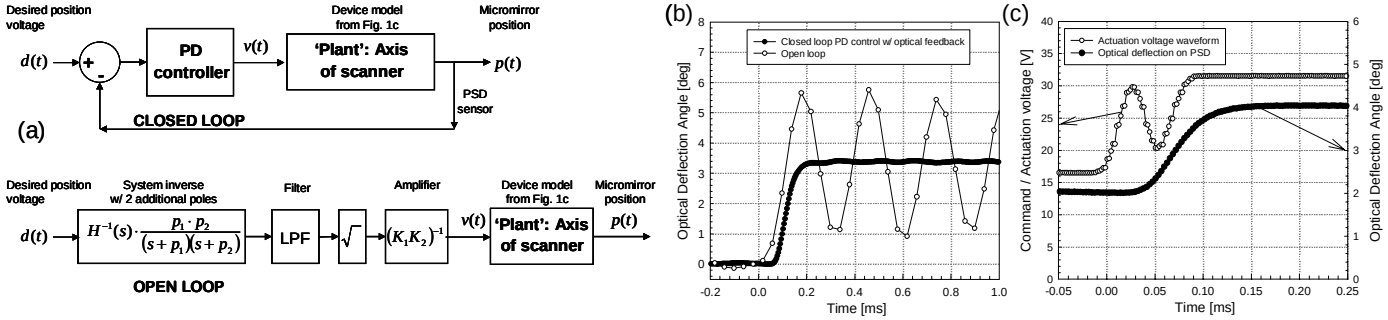

Figure 2. (a) Schematics of the closed-loop scheme with PD controller (CLPD) and below, the open-loop inverse square-root (ISR) scheme. For the ISR scheme, two additional high frequency poles p_1 and p_2 are added to obtain a stable and causal system. (b) Comparison of step response of Device 1 with and without the PD controller. Without the controller, settling time is ~20 ms, while with PD control settling time is 104 μs. (c) Best result of ISR scheme with Device2 with the actuation waveform and resulting step response both shown.

(a)

Settling Time [μs]	LPF Butterworth Order = 6 $\omega_p = \omega_n / 3.5$	LPF Bessel Order = 6 $\omega_p = \omega_n / 2.7$	LPF Bessel Order = 24 $\omega_p = \omega_n / 1.3$	ISR	CLPD
Device 1	376	440	292	128	104
Device 2	510	476	280	96	92
Device 3	1750	1050	790	284	N/A

(b)

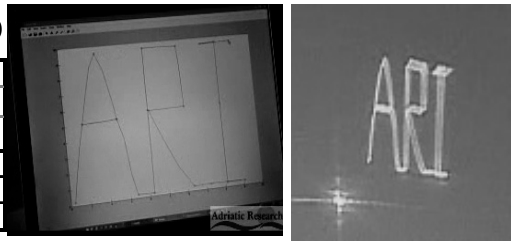

Figure 3. (a) Table of measured settling times for different devices and control schemes. The filter order and passband frequency ω_p for the Bessel and Butterworth filters are indicated. Settling time for the step response is defined as the time for the signal to settle to within 1% of the final value. In the ISR model, a Bessel filter of 13th order with ω_p = 25 kHz was used as the LPF block of Fig. 2a. (b) Example of a vector scanned pattern generated by our laptop demo system described below in Fig. 4. Pattern is displayed on the wall with a 40 Hz refresh rate. The patterns and filters were generated in MATLAB and the actuating voltages were applied through the audio port.

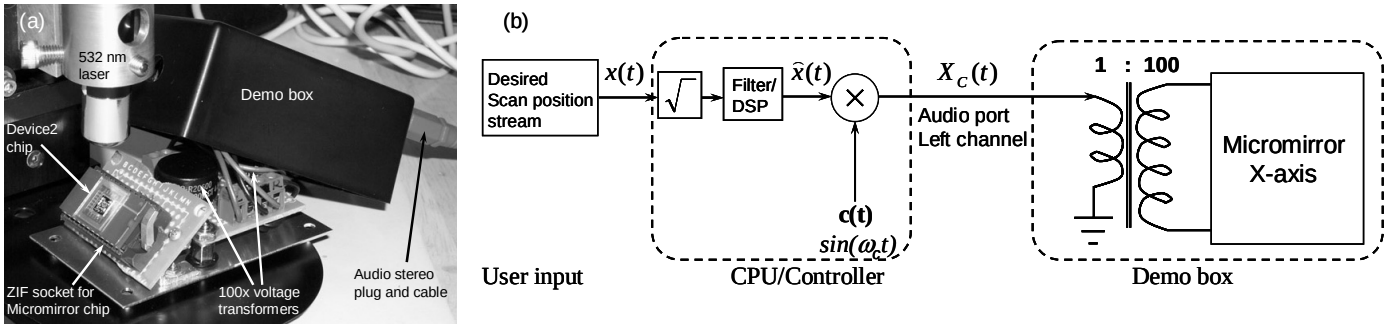

Figure 4. Low-voltage device operation methodology using a laptop's audio output port: (a) micromirror scanner is inserted in a demo box which includes 2 audio-transformers for 100:1 voltage gain and distributes audio L channel to X-axis actuators and audio R channel to Y-axis actuators. (b) desired user position input is transformed by square root function and proper low-pass filtering and then modulated to a carrier frequency (e.g. 17000 Hz). Audio transformer amplifies the voltage 100 times and delivers to the micromirror actuator. Same setup is present for the micromirror Y-axis, utilizing audio port's right channel.